

## LETTER

**Saliency-Guided Lighting**Chang Ha LEE<sup>†a)</sup>, Member, Youngmin KIM<sup>††</sup>, and Amitabh VARSHNEY<sup>††</sup>, Nonmembers

**SUMMARY** The comprehensibility of large and complex 3D models can be greatly enhanced by guiding viewer's attention to important regions. Lighting is crucial to our perception of shape. Careful use of lighting has been widely used in art, scientific illustration, and computer graphics to guide visual attention. In this paper, we explore how the saliency of 3D objects can be used to guide lighting to emphasize important regions and suppress less important ones.

**key words:** lighting design, mesh saliency, visual perception, enhancement

**1. Introduction and Related Work**

Recent advances in 3D model acquisition technologies have resulted in creation of gigantic meshes with millions to billions of points. The visual overload caused by the dramatically rising complexity of 3D models prevents us from effectively analyzing and understanding their visual depiction. Research in perceptual psychology has shown that a two-component framework controls where the human visual attention is deployed in visual scenes [1], [2]. The bottom-up mechanism guides the viewer's attention to stimulus-based salient regions. The contrast of colors, intensities, and orientations affects the salience for the bottom-up mechanism. The top-down visual attention involves semantic context for the scenes. Without any task-based knowledge for the scenes, viewers observe a scene in a bottom-up way. Naive rendering of complex models often produces a large amount of visual stimuli, especially when used with feature-enhancing lighting design techniques [3]–[6]. This defocuses visual attention, leading to a less effective understanding of the scene. Rensink *et al.* [7] have found that observers have difficulty in identifying changes in a scene unless their attention is drawn to the changed regions with verbal cues. Their experiments show that (a) the amount of visual information often exceeds our ability to perceive it effectively and (b) guiding visual attention helps to better analyze and understand the scene.

Braun [8] has found that directing the visual attention based on low-level visual cues as well as object saliency plays a significant role in visual search tasks. His experiments involved showing users several objects with different saliencies based on their size, contrast, and patterns. The

users' task was to find a target object among them. He found that a high-contrast object surrounded by low-contrast objects is more noticeable than a low-contrast object surrounded by high-contrast objects. His results show that enhancing the contrast of regions helps us perceive them better.

Several researchers have used contrast enhancement for enhancing important features in graphics data. Gooch *et al.* [9] have proposed a method for converting color images to grayscale images while preserving salient features. They maintain the luminance contrasts in a grayscale image to convey the differences in the CIE color space. Rasche *et al.* [10] have also presented a method for removing color while preserving image details by enhancing their contrast in grayscale images. Ehrlicke *et al.* [11] have developed an algorithm for visualizing vasculature from volume data by enhancing the contrast of line-like structures detected by pattern recognition techniques. Researchers have also used lighting to enhance contrast. Raskar *et al.* [12] have used multiple flashes to generate non-photorealistic images from photographs by detecting edges. They enhance contrast around silhouettes by using different flashlight directions for improved edge detection. Kachar [13] has proposed a method for improving the illumination of transparent objects in microscope images by enhancing contrast with an oblique light direction.

High contrast can sometimes lower the overall image quality. When the contrast in an image is too high, the regions with low luminance are not readily noticeable. Tone reproduction, or tone mapping, is a mapping from the real-world luminance intensities to the display luminance intensities [14]–[19]. Tone mapping is important because the dynamic range of current display devices is much lower than the real-world dynamic range. Therefore, a bright spot in an image such as bright sunlight coming from the window may make other regions appear too dark. In this case, suppressing contrast between bright regions and dark regions improves overall comprehensibility.

In this paper, we introduce *salient lighting* to emphasize salient regions by varying the illumination contrast range based on the computed saliency of the surface point. The observations of Cavanagh [20] suggest that we are insensitive to the global inconsistencies of illumination if the local lighting is consistent. The mesh saliency approach described in [21] can vary rapidly across an object. Applying that idea directly in a salient lighting approach may cause distracting lighting inconsistencies. To avoid this problem, we use a smoothed version of mesh saliency. We have also

Manuscript received April 24, 2008.

Manuscript revised September 24, 2008.

<sup>†</sup>The author is with the School of Computer Science and Engineering, Chung-Ang University, Korea.

<sup>††</sup>The authors are with the Department of Computer Science, University of Maryland, USA.

a) E-mail: chlee@cau.ac.kr

DOI: 10.1587/transinf.E92.D.369

experimented with a new saliency-computation method and use it for salient lighting for molecular visualization.

In molecular graphics, there are various tools for visualizing 3D protein models, including KiNG viewer [22], Jmol, WebMol, Protein Workshop, and QuickPDB [23]. These tools enable us to explore and understand 3D structures of proteins in various forms such as CPK, ball and stick, ribbons, and molecular surfaces. Also they provide useful options such as interactive controls, depth cues, and shadings for better understanding of 3D structures. Our method proposed in this paper complements to these tools since it estimates and highlights salient regions that might be important for understanding the functions and structures of the proteins. These salient regions are automatically found by detecting geometrically unique features that attract the human visual attention. Moreover, our method can emphasize user-defined salient regions in case users have their own definition of importance. In this case, our illumination method can be directly applied to the user-defined saliency without computing the saliency.

## 2. Salient Lighting Overview

In this section we discuss emphasizing salient regions based on their importance. This involves two steps. First, we define the regional importance, and second we determine how to emphasize salient regions.

In this paper, we use the computational mesh saliency approach as described in [21] as an estimate of the regional importance. We will like to note that for some applications where saliency is based on subjective semantics, it might be more appropriate to acquire it through direct user input. Research on lighting design has used interfaces to sketch the desired rendering result directly on the 3D models [24]–[26]. Recent techniques for drawing on the 3D meshes [27]–[29] could also facilitate building a system for acquiring the regional importance of 3D meshes through user interfaces.

There are many ways of emphasizing salient regions. As we discussed in Sect. 1, one can improve the comprehensibility by enhancing the contrast. We can apply this idea to improve the visualization of salient regions by enhancing the contrast in salient regions and suppressing it in non-salient regions. We can manage the contrast level of the illumination by suitably modifying ambient, diffuse, and specular lights, as well as material properties.

Another method for enhancing the contrast is to change colors based on the saliency. Gooch *et al.* [30] have proposed a non-photorealistic lighting model. They have used warm to cool tones in color transition along the surface-normal changes. This technique helps emphasize the depth cue since we perceive the regions with cool colors to be receded and warm-colored regions to be advanced. We could use this concept to accentuate salient regions in warm colors and suppress non-salient regions in cool colors.

In this paper, we experiment with a simple approach to show how we can emphasize salient regions by accentuating or attenuating the illumination including ambient, diffuse,

and specular lights based on the computed saliency.

## 3. Normal-Based Salient Lighting

One of the interesting applications for salient lighting is molecular graphics. We are interested in modeling and visualization of protein ion channels that regulate the flow of ions into and out of the cells. The visualization of macromolecular surfaces is challenging since they have rough surfaces due to the spherical representation of atoms. As seen in Fig. 1 (a), visualization of these surfaces under the traditional local illumination does not adequately reveal the overall structure of the molecule. Using the mesh saliency computed by the center-surround mechanism with mean curvature as in the previous section is also inadequate. For the *E. coli* membrane channel in Fig. 2, the curvature-based mesh saliency starts to show good results from the scale 8 Å and picks the oblique clefts on the side as salient, but fails to detect the central channel as salient. Figure 3 shows that the

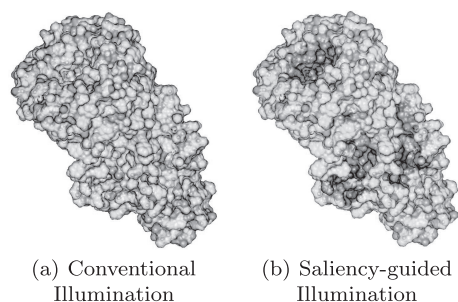


**Fig. 1** Rendering of *E. coli* membrane channel. Our saliency-guided rendering clearly shows the central channel as well as the oblique clefts on the side which are not readily apparent with traditional local illumination.

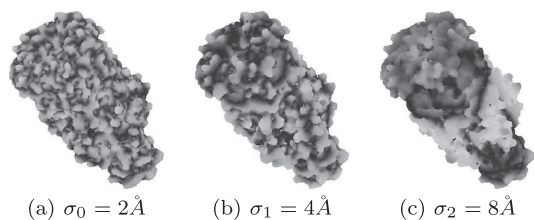


**Fig. 2** Figures show the saliency maps on the *E. coli* membrane channel at multiple scales  $\sigma_i$ . The size of the *E. coli* membrane channel is 54.59 Å × 54.81 Å × 96.82 Å.

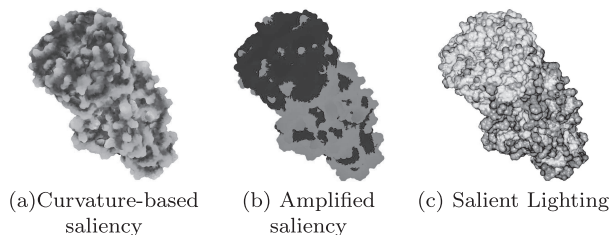


**Fig. 3** Salient lighting on *E. coli* membrane channel based on the saliency computed by applying a center-surround operator to the mean curvature.

salient lighting with the curvature-based saliency does not reveal the central channel.

For the vertices of the molecular surface along the walls of the central channel, the mean curvatures at small and large scales are largely similar but the average normal vectors are not. Therefore, the normal-based method is able to better detect the central channel and the oblique clefts on the side as salient. Thus, we apply the center-surround mechanism to normal vectors instead of mean curvature to saliently illuminate molecular surfaces. In this section, we define the salient region as the region where the distribution of its normal vectors are different from its surroundings.

To compute the difference between normal distributions, we fit planes to two point clouds of the neighborhood at fine and large scales using Principal Component Analysis (PCA) [31] and compute the angle between the normal vectors of the two planes. Figure 4 illustrates this operator. Let the normal map  $\mathcal{M}$  define a mapping from each vertex of a mesh to its normal vector, i.e. let  $\mathcal{M}(v)$  denote the normal vector of the vertex  $v$ . Let  $V(\mathcal{M}(v), \sigma)$  denote the normal vector of the plane fitted to the points that are within a distance  $\sigma$  from  $v$ . We define the saliency of a vertex  $v$  at a scale level  $i$  as  $\mathcal{S}_i(v)$ :

$$\mathcal{S}_i(v) = |\text{acos}(V(\mathcal{M}(v), \sigma_i) \cdot V(\mathcal{M}(v), 2\sigma_i))|$$

where,  $\sigma_i$  is the distance for generating neighboring points at scale  $i$ . We have used hierarchical scales  $\sigma_i \in \{2 \text{ \AA}, 4 \text{ \AA}, 8 \text{ \AA}\}$  for this example, and the nonlinearly aggregated mesh saliency  $\mathcal{S} = \sum_{i=0}^2 \mathcal{S}(\mathcal{S}_i)$ . We have also used the saliency amplification operator  $A(\mathcal{S}(v), \alpha, \lambda)$  as described in saliency-based simplification [21]. We use  $\lambda = 10$  and  $\alpha = 60^{\text{th}}$  percentile saliency. We use  $\sigma = 8 \text{ \AA}$  for blurring, i.e. the final saliency map  $\mathcal{S}_f = A(G(\mathcal{S}, 8 \text{ \AA}))$ .

We define a *salient weight map*  $\mathcal{W}$  as a weighting factor for emphasizing salient regions. Let  $s_{\min}$  and  $s_{\max}$  be the minimum and the maximum values of the final saliency map. We compute a salient weight  $\mathcal{W}(v)$  at a vertex  $v$  by mapping the final saliency value  $\mathcal{S}_f(v)$  into a range  $[a, b]$ :  $\mathcal{W}(v) = a + (\mathcal{S}_f(v) - s_{\min})(b - a)/(s_{\max} - s_{\min})$ . For the examples in this section, we use values  $a = 0$  and  $b = 0.3$ .

In this section, we use a constant ambient light and emphasize salient regions by darkening them, i.e. we multiply  $1 - \mathcal{W}$  to the diffuse and specular illumination for computing salient illumination.

We have also used multi-resolution techniques for efficiency. We simplified the molecular surface to 5%, 10%,

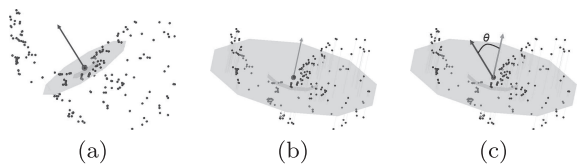


**Fig. 4** Figure (a) shows the plane fitted to the neighboring points at a fine scale and its normal vector, (b) shows the fitting plane and its normal vectors at a coarse scale, and (c) shows the angle between the two normal vectors.

and 20% of the initial number of triangles. We use Qslim [32] for simplification and keep track of the edge contractions so that we know each vertex in the original mesh is contracted to which vertex in the simplified mesh. Then we compute the saliency in the simplified mesh. The saliency in the original mesh is computed by mapping the saliency of contracted vertices to the saliency of original vertices.

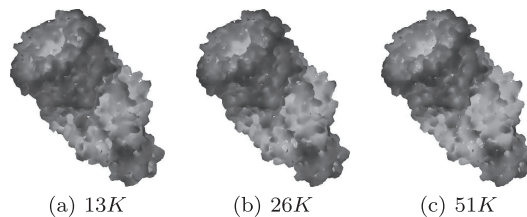
## 4. Results

Table 1 shows the times for computing saliency of *E. coli* membrane channel at different levels of detail, and Fig. 5 shows the saliency maps. It takes 2 hours 54 minutes 18 seconds for computing saliency of the original model with 234 K vertices at the scale 4 Å, while the simplified version with 26 K vertices takes 37.23 seconds. This gives us a factor of more than 280 speed-up by using a low-resolution mesh with barely any difference as seen in Fig. 5. Figure 6 (a) shows the original saliency without amplification, (b) shows the amplified saliency, and (c) shows the salient lighting with the saliency map shown in (b). As you can see, the salient lighting can clearly illuminate the central channel and the oblique clefts on the side while the traditional local illumination cannot (Fig. 1 (a)).

Figure 7 shows the results of saliency-guided lighting on several molecular structures. Figure 7 (a) shows a saliency-guided lighting on Ribonuclease A (5rsa). The

**Table 1** Run times for computing saliency of *E. coli* membrane channel.

#Verts	Time for each scale (sec)		
	2 Å	4 Å	8 Å
13K	2.00	10.34	49.67
26K	6.54	37.23	206.06
51K	24.51	146.61	929.71



**Fig. 5** Figures show the saliency maps on the *E. coli* membrane channel at multiple levels of detail.

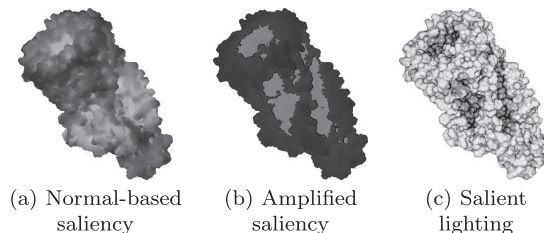


**Fig. 6** Salient lighting on *E. coli* membrane channel based on the saliency computed by applying a center-surround operator to the normal vectors.

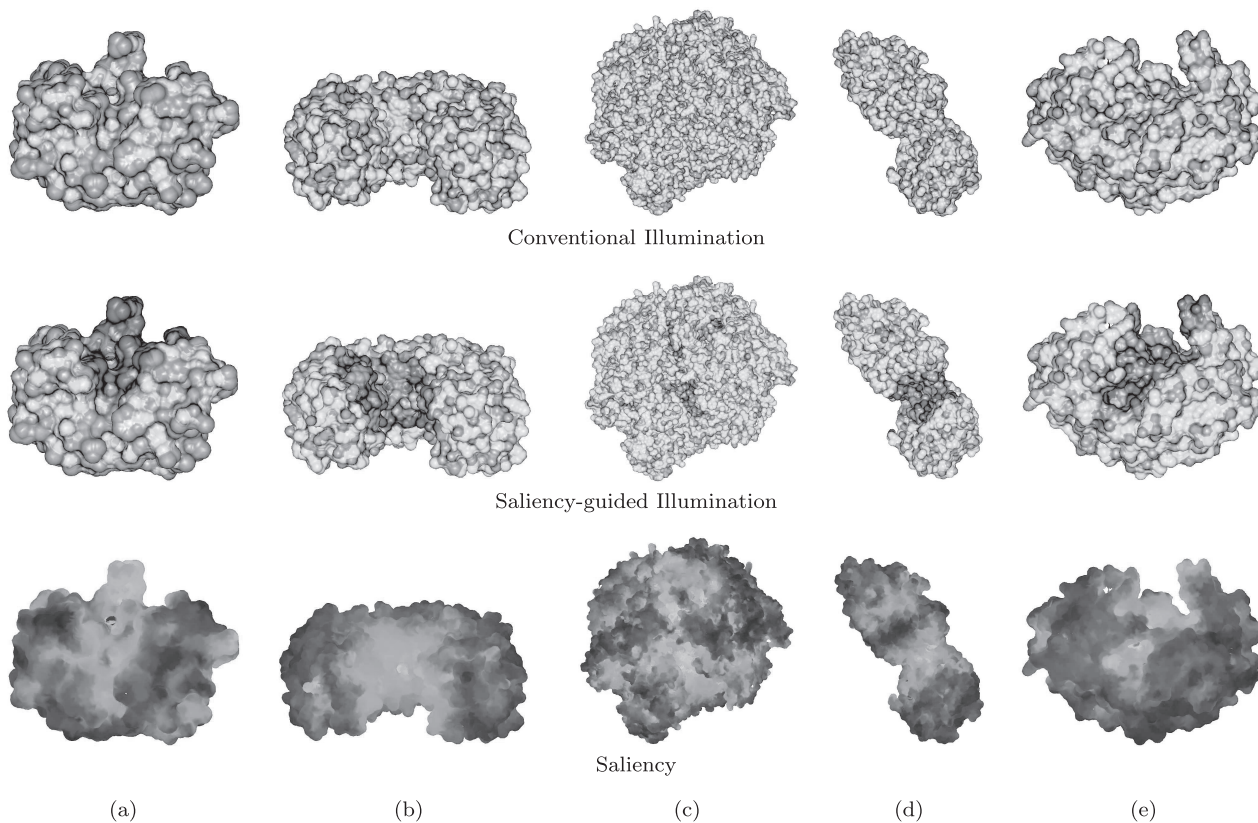


**Fig. 7** Salient lighting on various models: (a) Ribonuclease A (5RSA). The size is  $35.80 \text{ \AA} \times 46.29 \text{ \AA} \times 33.36 \text{ \AA}$  (b) Ribonuclease inhibitor (2BNH). The size is  $61.35 \text{ \AA} \times 66.45 \text{ \AA} \times 60.76 \text{ \AA}$  (c) Exosomes (2NN6). The size is  $116.26 \text{ \AA} \times 111.72 \text{ \AA} \times 113.85 \text{ \AA}$  (d) Antibody Hulysl Fv (1BVL). The size is  $76.07 \text{ \AA} \times 64.59 \text{ \AA} \times 57.70 \text{ \AA}$  (e) Pepsin (5PEP). The size is  $44.59 \text{ \AA} \times 48.84 \text{ \AA} \times 62.07 \text{ \AA}$

middle image illuminates the groove in the top center area, where the RNA chain fits and is attacked by a collection of acidic and basic amino acids [23]. The Ribonuclease inhibitor (2BNH) shown in (b) is a receptor to the Ribonuclease A. The salient lighting on Ribonuclease inhibitor emphasizes its docking site as shown in the middle image. The image (c) shows the result on Exosomes (2NN6). The saliency-guided lighting in the middle image elucidates the central holes of Exosomes. Antibody Hulysl Fv (1BVL) shown in (d) is a receptor to the Lysozyme. The saliency-guided lighting illuminates the docking site of Antibody Hulysl Fv to the Lysozyme. Pepsin (5PEP) shown in (e) is the first one in a series of enzymes that digest proteins in the stomach. The groove highlighted in the middle image is the deep active site that binds protein chains and breaks them into smaller pieces [23].

## 5. Conclusion

In this paper, we have proposed a saliency-guided modification of the lighting pipeline to emphasize salient regions. Our approach varies the illumination of a vertex based on its saliency. Salient regions are emphasized with a salient light which is darker or brighter than the lighting on non-salient regions. We have also extended the model of mesh

saliency [21] for emphasizing salient regions with saliency-guided illumination. We have used center-surround operators with PCA-analyzed normal vectors for dealing with bumpy surfaces in molecular graphics. Our salient lighting can illustrate global geometric structures such as the central channel and the side oblique clefts in the *E. coli* membrane channel.

## Acknowledgements

This work was supported in part by the NSF grants: IIS 04-14699, CCF 04-29753, CNS 04-03313, and CCF 05-41120. It was also supported partially by a grant (CR070019) from Seoul R&BD Program funded by the Seoul Development Institute of Korean government and the NRL Program (Grant ROA-2008-000-20060-0) from the Korea Science & Engineering Foundation.

## References

- [1] L. Itti and C. Koch, "Computational modelling of visual attention," *Nature Reviews Neuroscience*, vol.2, no.3, pp.194–203, 2001.
- [2] D. Parkhurst, K. Law, and E. Niebur, "Modeling the role of saliency in the allocation of overt visual attention," *Vision Research*, vol.42, no.1, pp.107–123, 2002.

- [3] S. Gumhold, "Maximum entropy light source placement," *Proc. IEEE Visualization*, pp.275–282, 2002.
- [4] C.H. Lee, X. Hao, and A. Varshney, "Light collages: Lighting design for effective visualization," *Proc. IEEE Visualization*, pp.281–288, 2004.
- [5] C.H. Lee, X. Hao, and A. Varshney, "Geometry-dependent lighting," *IEEE Trans. Vis. Comput. Graphics*, vol.12, no.2, pp.197–207, 2006.
- [6] R. Shacked and D. Lischinski, "Automatic lighting design using a perceptual quality metric," *Computer Graphics Forum (Eurographics 2001)*, vol.20, no.3, pp.215–226, 2001.
- [7] R. Rensink, J. O'Regan, and J. Clark, "To see or not to see: The need for attention to perceive changes in scenes," *Psychological Science*, vol.8, no.5, pp.368–373, 1997.
- [8] J. Braun, "Visual search among items of different salience: Removal of visual attention mimics a lesion in extrastriate area V4," *J. Neuroscience*, vol.14, no.2, pp.554–567, 1994.
- [9] A. Gooch, S. Olsen, J. Tumblin, and B. Gooch, "Color2Gray: Saliency-preserving color removal," *ACM Trans. Graphics (SIGGRAPH 2005)*, vol.24, no.3, pp.634–639, 2005.
- [10] K. Rasche, R. Geist, and J. Westall, "Detail preserving reproduction of color images for monochromats and dichromats," *IEEE Comput. Graph. Appl.*, vol.25, no.3, pp.22–30, 2005.
- [11] H.H. Ehrlicke, K. Donner, W. Koller, and W. Straßer, "Visualization of vasculature from volume data," *Comput. Graph.*, vol.18, no.3, pp.395–406, 1994.
- [12] R. Raskar, K. Tan, R. Feris, J. Yu, and M. Turk, "Non-photorealistic camera: Depth edge detection and stylized rendering using multi-flash imaging," *ACM Trans. Graphics (SIGGRAPH 2004)*, vol.23, no.3, pp.679–688, 2004.
- [13] B. Kachar, "Asymmetric illumination contrast: A method of image formation for video light microscopy," *Science*, vol.227, no.4688, pp.766–768, 1985.
- [14] M. Ashikhmin, "A tone mapping algorithm for high contrast images," *Eurographics Workshop on Rendering*, pp.1–11, 2002.
- [15] F. Durand and J. Dorsey, "Fast bilateral filtering for the display of high dynamic range image," *Proc. ACM SIGGRAPH*, pp.257–265, 2002.
- [16] R. Fattal, D. Lischinski, and M. Werman, "Gradient domain high dynamic range compression," *Proc. ACM SIGGRAPH*, pp.249–256, 2002.
- [17] S.N. Pattanaik, J.A. Ferwerda, M.D. Fairchild, and D.P. Greenberg, "A multiscale model of adaptation and spatial vision for realistic image display," *Proc. ACM SIGGRAPH*, pp.287–298, 1998.
- [18] E. Reinhard, M. Stark, P. Shirley, and J. Ferwerda, "Photographic tone reproduction for digital images," *Proc. ACM SIGGRAPH*, pp.267–276, 2002.
- [19] J. Tumblin and G. Turk, "LCIS: A boundary hierarchy for detail-preserving contrast reduction," *Proc. ACM SIGGRAPH*, pp.83–90, 1999.
- [20] P. Cavanagh, "Pictorial art and vision," *MIT Encyclopedia of the Cognitive Sciences*, pp.644–646, 1999.
- [21] C.H. Lee, A. Varshney, and D. Jacobs, "Mesh saliency," *ACM Trans. Graphics (SIGGRAPH 2005)*, vol.24, no.3, pp.659–666, 2005.
- [22] KiNG Viewer. <http://kinimage.biochem.duke.edu/>
- [23] RCSB Protein Data Bank. <http://www.rcsb.org/>
- [24] P. Poulin and A. Fournier, "Lights from highlights and shadows," *Symposium on Interactive 3D Graphics*, pp.31–38, 1992.
- [25] P. Poulin, K. Ratib, and M. Jacques, "Sketching shadows and highlights to position lights," *Proc. Computer Graphics International*, pp.56–64, 1997.
- [26] C. Schoeneman, J. Dorsey, B. Smits, J. Arvo, and D. Greenberg, "Painting with light," *Proc. ACM SIGGRAPH*, pp.143–146, 1993.
- [27] W. Baxter and M. Lin, "A versatile interactive 3D brush model," *Proc. Pacific Graphics*, pp.319–328, 2004.
- [28] R.D. Kalnins, L. Markosian, B.J. Meier, M.A. Kowalski, J.C. Lee, P.L. Davidson, M. Webb, J.F. Hughes, and A. Finkelstein, "WYSIWYG NPR: Drawing strokes directly on 3D models," *ACM Trans. Graphics (SIGGRAPH 2002)*, vol.21, no.3, pp.755–762, July 2002.
- [29] Y. Kho and M. Garland, "User-guided simplification," *Symposium on Interactive 3D Graphics*, pp.123–126, 2003.
- [30] A. Gooch, B. Gooch, P. Shirley, and E. Cohen, "A non-photorealistic lighting model for automatic technical illustration," *Proc. ACM SIGGRAPH*, pp.447–452, 1998.
- [31] R.O. Duda, P.E. Hart, and D.G. Stork, *Pattern Classification*, 2nd ed., John Wiley & Sons, New York, 2001.
- [32] M. Garland and P. Heckbert, "Surface simplification using quadric error metrics," *Proc. ACM SIGGRAPH*, pp.209–216, 1997.
-